Scientia Iranica F (2022) 29(6), 3543–3553

SCIENTIA IRANICA

Sharif University of Technology
Scientia Iranica
Transactions F: Nanotechnology
http://scientiairanica.sharif.edu

Experimental study of effect of laser machining process of CO_2 on electrical conductivity and magnetic properties of PMMA/MWCNT composite

S. Jabbarpour Azari[a] and M. Aali[b,*]

a. *Department of Mechanical Engineering, Tabriz Branch, Islamic Azad University, 5157944533, Tabriz, Iran.*
b. *Institute for Polymers and Composites (IPC), Department of Polymer Engineering, Campus of Azurém, University of Minho, 4800-058 Guimarães, Portugal.*

Received 31 March 2020; received in revised form 20 November 2021; accepted 3 January 2022

KEYWORDS
Nano-composite;
Polymethyl methacrylate (PMMA);
Multi-wall carbon nanotubes (MWCNT);
Electrical resistance;
Magnetic properties.

Abstract. This study aims to investigate the effect of such parameters as laser machining process and laser line angle to injection direction of sample plastics on the electrical resistance of Polymethyl Methyl Methacrylate (PMMA)/Multi-Wall Carbon Nanotubes (MWCNT) nanocomposite. The laser machining process was applied to the samples considering a combination of power, feed rate, and laser line angle with respect to the direction of melted flow parameters. According to the obtained results from measurements of electrical resistance and magnetic properties, it was found that the laser line angle to the direction of melted flow did not statistically and physically affect the electrical resistance of the composite. Moreover, increasing the laser machining power led to reduction of electrical resistance. On the other hand, feed rate enhancement (with fixed lasering power) increased the electrical resistance. Moreover, it was determined that laser machining did not significantly affect the magnetic properties of the samples.

1. Introduction

During the last decade of the 20th century, a new field known as a nanocomposite entered composites science and technology. Nanocomposites are compound materials and at least, one of their components has nanometer dimensions (1–100 Nm). In recent years, nanocomposites significantly progressed in comparison to composite materials on conventional scales due to varying combinations, structure of nanometer materials, and unique properties [1,2].

The application of carbon nanotubes to metal-based composites has been recently prevalent. Carbon nanotubes have unique physical and mechanical properties such as high electrical and thermal conductivity as well as very high strength and elastic modulus. Carbon nanotubes have been selected as ideal amplifiers in fabricating nanocomposites in order to improve their properties relying on the mentioned properties. The most important challenge in developing metal nanocomposites amplified with nanotubes is preventing their clustering in production processes, reaching their uniform distribution in the background, and creating superficial bonds between carbon nanotubes and metal backgrounds [1–3].

Few studies have recently been conducted on physical properties such as electrical conduction, especially the magnetic behavior of composites containing

*. *Corresponding author. Tel: +98 41 34417269*
E-mail addresses: salarazari68@gmail.com (S. Jabbarpour Azari) and Aali@dep.uminho.pt (M. Aali)

doi: 10.24200/sci.2022.55724.4374

carbon nanotubes. It is important to investigate the role of carbon nanotubes in the magnetic and electrical behaviors of such composites [4].

Furthermore, several studies have been conducted concerning the effect of the laser machining process on polymer-based nanocomposites [5]. Ghavidel et al. [5] investigated cutting quality and electrical resistance of PMMA/MWCNT nanocomposite using different parameters of laser machining process (power and feed rate) and different percentages of MWCNT. Won Gee et al. [6] presented the effect of different percentages of carbon nanotubes on mechanical properties of PMMA/MWCNT composite and found that more than 1% increase in the mass of carbon nanotubes would lead to the reduction of mechanical properties in the final material. Different lasering parameters and different percentages of carbon nanotubes were presented by Karimzad Ghavidel et al. [7]. According to their study, uniform distribution of carbon nanotubes in the alloy background enhanced the electrical properties of nanocomposites. In another work, Davim et al. [8] investigated the cutting quality of polymer materials using power and feed rate parameters of the CO_2 laser machining process. They found that the heat-affected zone increased upon increasing the laser power and decreased with increase in feed rate. Moraczewski et al. [9] used laser, chemical, and plasma machining processes to machine polylactide surfaces. Following laser machining, Liebscher et al. [10] investigated the conductivity of polypropylene/polycarbonate filled with nanotubes. Gan et al. [11] scrutinized the difference between conductivity and mechanical properties of MWCNT/SWCNT. Yuan et al. [12] determined that laser-separated microstructures increased electrical conductivity. Ning et al. [13] studied the effect of fillers and their combination methods on electrical conductivity. Kim and Lee [14] analyzed the effect of different laser parameters on surface smoothness and cutting quality. Ajay Kumar Sharma et al. [15] studied the dielectric properties and thermal stability of MWCNT composites. Wang et al. [16] concluded that the properties of composites including MWCNT and parameters affected their electrical conductivity and magnetic properties. Kumar et al. [17] investigated the mechanical and structural properties due to the addition of MWCNT. G.B. The effect of different methods of homogeneous distribution of CNTs that improved the electrochemical properties was evaluated by Kunde et al. [18]. Arrechea et al. [19] examined the mechanical and structural changes of the composites by adding MWCNT. The effects of the addition of carbon nanotubes on the electrical conductivity of composites were investigated by Chayad et al. [20].

Achievement of the ideal electrical conductivity is an important objective of nanocomposites, especially polymer-based nanocomposites amplified by MWCNT. However, to achieve appropriate electrical conductivity, a second process such as laser machining process should be applied to them after producing nanocomposite [21]. In the polymer-based nanocomposites amplified by MWCNT, the relation between based polymer and MWCNT may be supposed as an electrical resistance chain in parallel and series forms, as depicted in Figure 1(a) [22]. This relation is promoted through

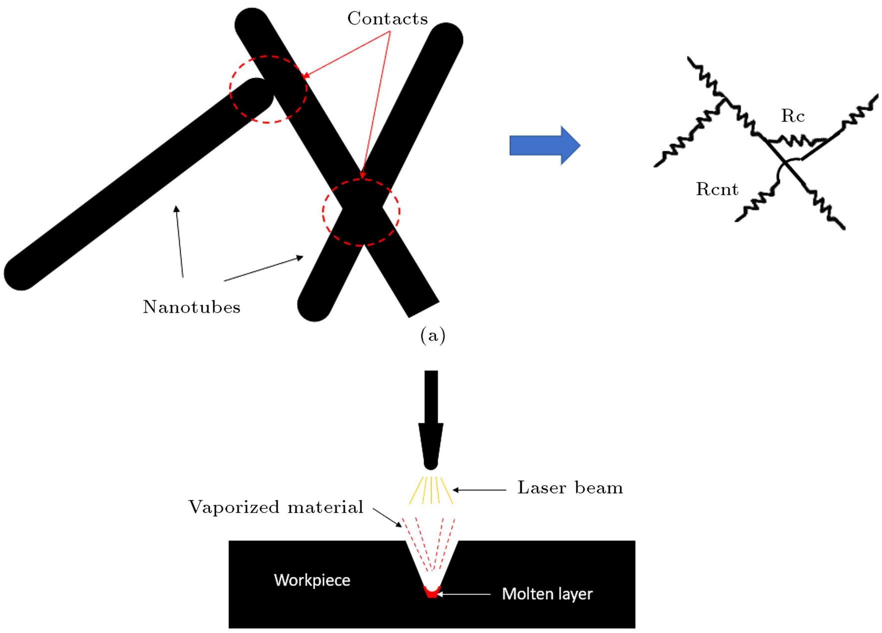

Figure 1. (a) Simulation of the location of carbon nanotubes inside the composite. (b) A schematic representation of the laser machining process.

the laser machining process such that the effect of laser machining is evidently seen on the reduction of electrical resistance. The effect varies at different angles of laser line to injection casting melted flow. If the angles are imposed manually, the laser machining process is continuous. However, if the angle is imposed by the Computer Numerical Control (CNC) method, laser rays will move step by step [21].

2. Experimental tests

2.1. Materials

In the present work, nanocomposite samples were produced through plastic injection casting. Then, the laser machining process was performed on the samples, as depicted in Figure 1(b), with a combination of power (at two levels of 10 and 40 W), feed rate (at three levels of 15, 45, and 75 m/m), and laser line angle to the direction of melted flow parameters (at six levels of 0, 18, 36, 54, 72, and 90 degrees). Laser line angle to the direction of melted flow was regulated by two manual and CNC methods. To measure magnetic properties, parameters of power (at two levels of 10 and 40 W) and feed rate (at three levels of 15, 45, and 75 m/m) were considered in the form of a square ring on CO_2 laser machining samples. Therefore, 72 tests were done to measure electrical resistance and 6 tests to measure magnetic properties (the number of variable parameters is 72).

The samples required for tests were supplied from the market. The samples are of PMMA/MWCNT type and 1% of their weight consists of MWCNT inside the matrix (polymethyl methacrylate). The sample size is 8×17 cm cut into six parts of 15×80 mm. Figure 2 depicts one of the six cut parts. The parts were made ready to measure electrical resistance. To test magnetic properties, six cube samples (5 mm) were cut from the main piece. Table 1 refers to the specifications of MWCNT used in this study, as depicted in Figure 3.

To measure electrical resistance using the designed probes, electrical resistance data were presented

Figure 2. A representation of the sample after the test.

Table 1. Specifications of MWCNT used in the present work.

Characteristic	Amounts
Purity	>95%
Outside diameter	30–50 nm
Inside diameter	5–15 nm
Length	10–20 mm
SSA	90–120 m^2/g
True density	~2.1 g/cm^3
Aspect ratio	200–666

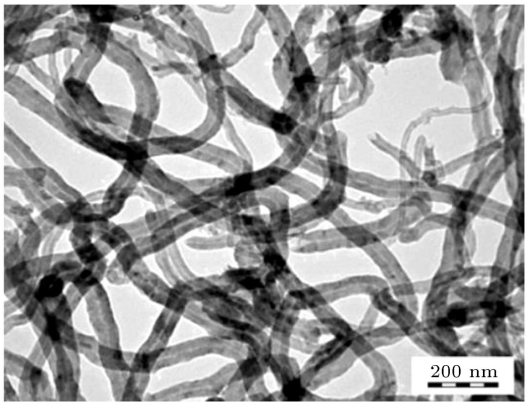

Figure 3. Images of transmission electronic microscope from MWCNT [26].

for both laser machining techniques (manual and CNC). To reduce the number of mistakes, electrical resistance was measured three times and the average was regarded as the electrical resistance of the sample.

FE-SEM was employed to observe changes of carbon nanotubes inside composite arising from the laser machining process on samples. Table 2 indicates EDX test results of a part of nanocomposites confirming MWCNT, as depicted in Figure 4.

2.2. Laser machining process

A laser system (CM1328 model) consisting of a laser source of 120 W and continuous CO_2 gas was applied to the laser machining process. The system consists of two numerical control axes in X and Y directions. Laser ray was used at 0, 18, 36, 54, 72, and 90 angle degrees to the direction of the melted flow on the pieces. The mentioned angles were used for laser machining of the pieces in both manual and CNC techniques.

2.3. Measurement of electrical resistance

After laser machining of nanocomposite samples, the electrical resistance of laser lines was measured using a digital multimeter. In the measuring process, the platinum probe was applied. The distance between these two designed probes was 10 mm. Figure 5 depicts a schematic of the platinum probe.

2.4. Measurement of mechanical properties

The magnetometer of the vibrating sample (made in

Table 2. Specifications of point EDX test of the sample in a 41.5-μm view field.

	Line	Int	Error	K	Kr	W%	A%	ZAF	Ox%	Pk/Bg	Class	LConf	HConf	Cat#
C	Ka	1072.5	93.553	1.000	1.000	100.0	100.0	1.000	0.00	264.21	A	98.43	101.57	0.00

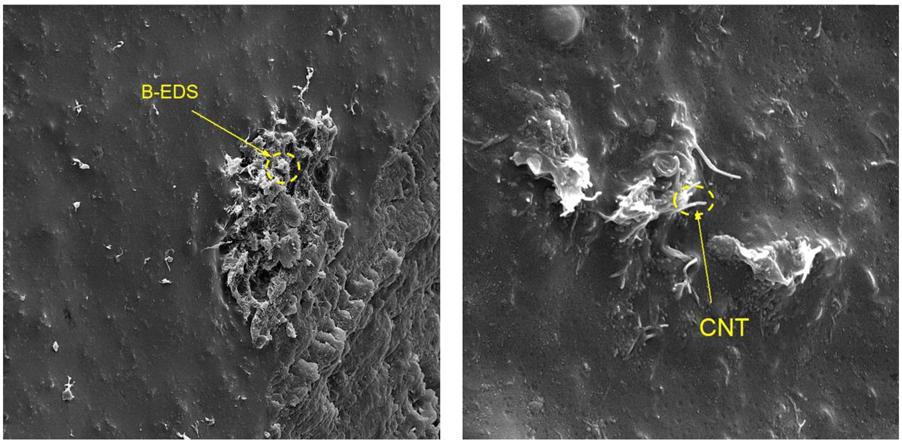

Figure 4. Location of EDX test in a 41.5-μm view field.

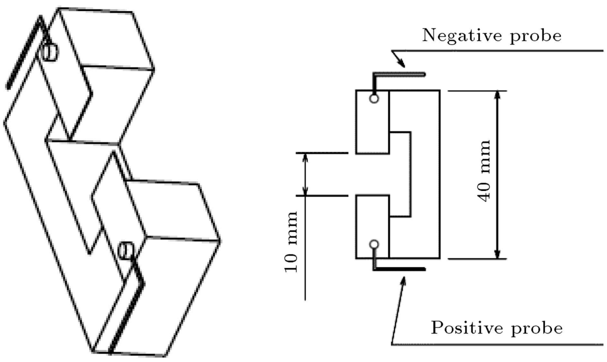

Figure 5. The fixture designed to measure electrical resistance.

USA • VSM oscillation frequency (calibrated): 1–100 Hz oscillation amplitude range of 0.1–5 mm sample size up to 6 mm diameter sensitivity parameters (RMS)) was used to measure magnetic properties of the samples after their laser machining. The system is capable of producing a field by 2T, which is ideal to measure the magnetic properties of the mentioned material. The system is used to measure magnetic parameters of materials (M-H curve) and extraction of other required data related to properties of magnetic materials and their performance in severe magnetic fields. The system provides the most complete data about magnetic properties. The laser machining process was repeated three times to lessen the number of possible mistakes in the test. Then, the average of these three data was computed for each parameter and the final result was recorded as the acquired data.

2.5. Test plan

In the present study, the power of the laser machining process was considered at two levels (10 and 40 W), laser feed rate at three levels (15, 45, and 75 mm/s), and laser line angle to the direction of melted flow at six levels (0, 18, 36, 54, 72, and 90 degrees). In selecting power levels of laser machining, only two levels (10 and 40 W) were satisfied due to lasering system restrictions and complete cutting of the piece in case of increasing the power to more than 40 W and inefficiency on the piece in case of reducing power to less than 10 W.

Table 3. Parameters of the laser machining process.

Levels	1	2	3	4	5	6
Angel (°)	0	18	36	54	72	90
Power (W)	10	40	-	-	-	-
Feed rate (mm/s)	15	45	75	-	-	-

The tests were designed using the complete factorial method. Thus, 75 tests were done and parameters of the laser machining process and its levels are summarized in Table 3 (If the power level exceeded 40, a complete cut would occur; if it was less than 10, it would not affect the sample.)

To measure magnetic properties, the samples were cut into 5 mm pieces by laser machining and fixed power. Then, the power of the laser machining process at two levels (10 and 40 W) and laser feed rate at three levels (15, 45, and 75 mm/s) was imposed on the samples in the form of a 3-mm square loop inside these laser machining pieces. A schematic of laser machining is shown in Figure 6.

3. Results and discussion

Data variance analysis was carried out to compare the efficiency of parameters in electrical resistance. A

Table 4. Variance analysis for conditions of angle impose using CNC.

Source	CR	P	F	MS	SS	DF
Power	46.2%	0.000	167.85	5943844	5943844	1
Feed rate	26.4%	0.000	48.06	1701908	3403815	2
Angle	-	0.087	2.67	94715	473575	5
Power × feed rate	10%	0.000	18.18	643616	1287231	2
Power × angle	9%	0.007	6.31	223385	1116925	5
Feed rate × angle	-	0.615	0.83	29281	292810	10
Error	-	-	-	35412	354120	10
Total	-	-	-	-	12872321	35

Table 5. Variance analysis for conditions of manual angle impose.

Source	CR	P	F	MS	SS	DF
Power	26.3%	0.000	62.85	2370060	2370060	1
Feed rate	47.8%	0.000	57.09	2152665	4305329	2
Angle	-	0.143	2.14	80733	403665	5
Power × feed rate	5%	0.012	7.16	269959	539918	2
Power × angle	-	0.058	3.15	118612	593059	5
Feed rate × angle	-	0.428	1.13	42448	424484	10
Error	-	-	-	37710	377096	10
Total	-	-	-	-	9013612	35

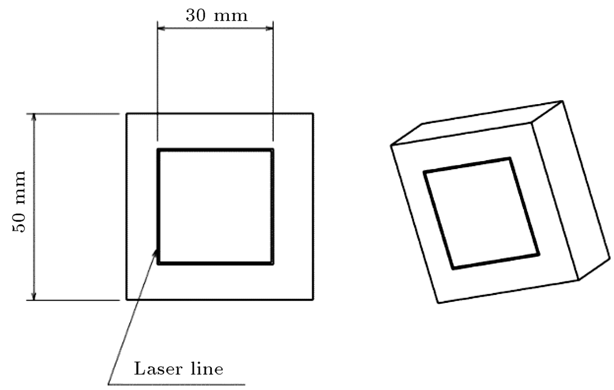

Figure 6. A schematic representation of laser machining for testing magnetic properties.

signal diagram was used to obtain the noise of the parameters at an optimized level and it was validated using average rate diagrams.

The variance of the obtained data was analyzed using Minitab software in order to study the effect of laser machining process parameters on the electrical resistance of laser lines. Using the P-factor, the parameters with physical and statistical effects on the electrical resistance of laser lines were introduced in this method. A parameter with a P-factor less than 0.05 has physical and statistical effects on electrical resistance with an error probability of 5% and a certainty probability of 95% in the process. Moreover, a CR column was designed for parameters with $P < 0.05$. CR parameter is calculated using Eq. (1). The parameter refers to the relative efficiency of each output parameter of the process:

$$CR = \frac{The\ Sum\ of\ Squares\ (SS)}{The\ total\ Sum\ of\ Squares\ (total\ SS)}. \quad (1)$$

Table 4 refers to variance analysis of the data obtained under conditions of angle impose using CNC. According to Table 4, the parameters of power, feed rate, power × feed rate, and power × angle (interaction of power and laser line angle with the direction of melted flow) had physical and statistical effects on the process output; i.e., the relative effect of power, feed rate, power × feed rate, and power × angle are 46.2%, 36.4%, 10%, and 9%, respectively. Table 5 refers to variance analysis of data obtained under conditions of manual angle impose. The parameters of power, feed rate, power × feed rate, and power × angle (interaction of power and laser line angle with the direction of melted flow) had physical and statistical effects on the process output; i.e., relative effect of power, feed rate, and power × feed rate were 26.3%, 47.8%, and 5%, respectively.

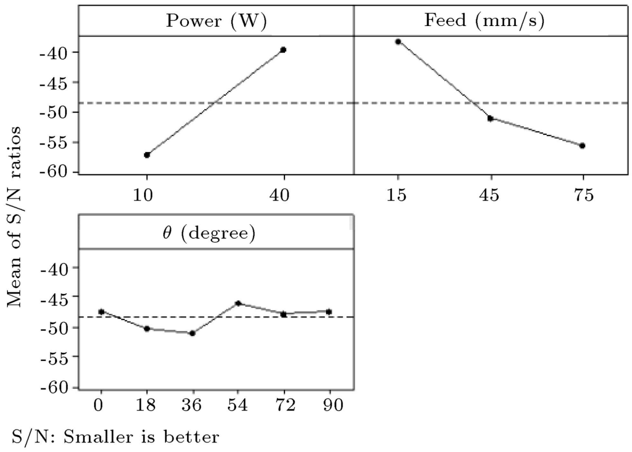

Figure 7. Signal-to-noise diagram of laser machining data imposed using CNC technique.

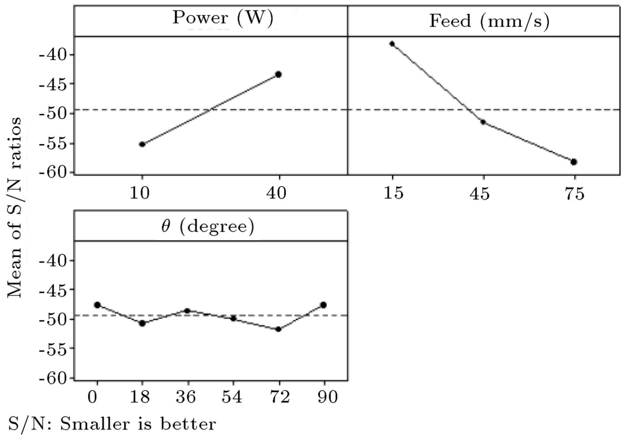

Figure 8. Signal-to-noise diagram of laser machining data imposed manually.

According to Tables 4 and 5, power $\times$ angle is physically and statistically effective only if the angle is imposed using the CNC technique. The reason may be attributed to the difference of laser live movement in two methods of angle impose, i.e., laser lines move continuously and straightly in the manual method while it moves in steps (combination of vertical and horizontal lines with very fine steps) in CNC technique. Therefore, the laser lines created in the CNC technique are longer than continuous and straight laser lines. In this case, more nanotubes are located beside each other and larger clusters are formed. It may be stated that laser machining using CNC technique is more effective in the electrical resistance of the laser line than the manual method.

The irregular and ambiguous effect of the angle between the laser line and melted flow may be attributed to the irregular distribution of MWCNT. Since the nanocomposites are produced using the plastic injection method, MWCNTs were distributed in the nanocomposite irregularly and in random directions. Thus, no specific relation may be obtained between the number of created connections in MWCNT and the angle between the laser line and the direction of the melted flow. Figure 7 depicts a signal diagram to laser machining data noise imposed using the CNC technique. As seen, the parameters of power and feed rate have the highest signal-to-noise ratio at levels of 40 W and 15 mm/s, respectively. Thus, the mentioned levels are introduced as the optimized levels, leading to minimum electrical resistance.

Figure 8 depicts a signal diagram-to-noise to impose a manual angle. As observed earlier, the parameters of power and feed rate have the highest signal-to-noise ratio at levels of 40 W and 15 mm/s, respectively. Thus, the mentioned levels are introduced as the optimized levels, leading to minimum electrical resistance.

General results of the effect of different laser

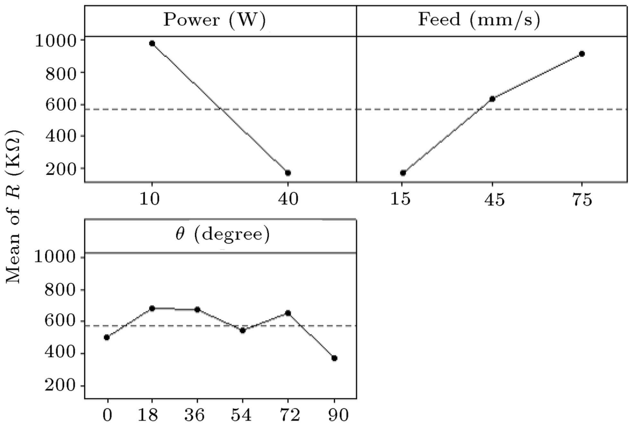

Figure 9. Average resistance diagram for conditions imposed using CNC technique.

machining parameters on electrical resistance indicate that increased laser power by 40 W leads to increase in cut depth so much so that it does not result in complete cut of the piece, improves the cluster size for nanotubes, and electron transfer in Hopping method, resulting in the reduction of electrical resistance. On the other hand, reduction of feed rate leads to increase in cut depth so much so that it does not result in complete cut of the piece and decrease in the electrical resistance since it results in increasing the size of the nanotube clusters.

Figure 9 depicts the average data of the laser machining process imposed using the CNC technique. As observed earlier, the power of 40 W and a feed rate of 15 mm/s have the minimum average rate of electrical resistance corresponding to signal-to-noise analysis. Moreover, the minimum average rate obtained for the angle between laser line and melted flow occurs at a level of 900° while the optimized level obtained from the signal-to-noise analysis is 54° for this parameter. Since power and feed rate parameters are physically and statistically effective, the statistically optimized level may be obtained. However, since the parameter

Table 6. Data of saturated magnetization parameter.

Power (W)	Feed rate (mm/s)	M_s (emu/g × E-6)			
		First measurement	Second measurement	Third measurement	The average value
10	15	4641.6	4341.3	4442.3	4475.1
10	45	4226.9	4456.1	5124.3	4602.5
10	75	4093.4	4953.7	4732.9	4593.3
40	15	4743.3	4373.2	4213.2	4443.2
40	45	4283.9	4515.1	4658.7	4485.9
40	75	4138.5	4711.2	4635.1	4495.1

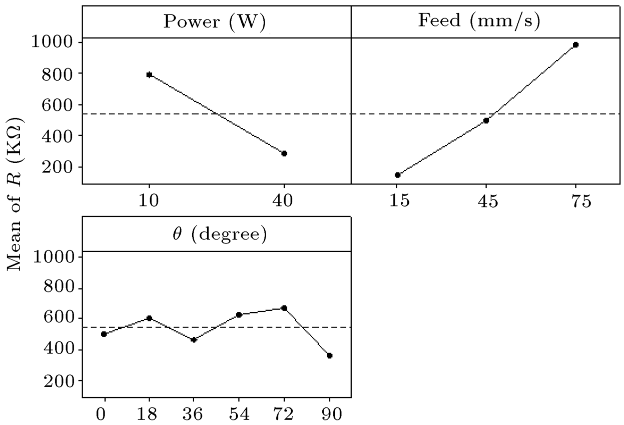

Figure 10. Average resistance diagram for manual angle impose.

of the angle between laser line and melted flow is not physically and statistically effective, the optimized level may not be obtained from the average rate and signal-to-noise diagrams. In other words, the parameter of the angle between laser line and melted flow does not have any regular effect on electrical resistance.

Figure 10 depicts the average laser machining process data imposed manually. As can be implied, the power of 40 W and feed rate of 15 mm/s have the minimum average rate of electrical resistance corresponding to signal-to-noise analysis. Furthermore, the minimum average rate obtained for the angle between laser line and melted flow occurs at a level of 90°, while the optimized level obtained from signal-to-noise analysis is 0° for this parameter.

It may be concluded that since power and feed rate parameters are physically and statistically effective, the statistically optimized level may be obtained. However, since the parameter of the angle between laser line and melted flow is not physically and statistically effective, the optimized level may not be obtained from the average rate and signal-to-noise diagrams. In other words, the parameter of the angle between laser line and melted flow does not have any regular effect on electrical resistance.

The irregular and ambiguous effect of the angle between the laser line and melted flow may be attributed to the irregular distribution of MWCNT. Since the nanocomposites are produced using the plastic injection method, MWCNTs were distributed in the nanocomposite irregularly and in random directions. Thus, no specific relation may be obtained between the number of the created connections in MWCNT and the angle between the laser line and the direction of the melted flow.

After imposing laser machining parameters mentioned in Figure 8, the samples were tested using a magnetometer of the vibrating sample. To study the data process, the average rate diagram was drawn for the saturated magnetization parameter. Table 6 shows the data obtained for the saturated magnetization parameter.

Upon studying the conductivity mechanism of nanocomposites containing MWCNT, it was concluded that addition of nanotubes to the inside of nanocomposites enhanced conductivity among their components such that a conductor network would be created between amplifier particles of the nanocomposite and the matrix. In the nanocomposites containing MWCNT, the conductivity network leads to electron transfer via two methods of quantum tunneling and hopping between the close nanotubes [23]. Quantum tunneling refers to the quantum process of particle tunneling along a barrier where the particle cannot pass it classically. Thus, this type of electron transfer occurs when the distance between carbon nanotubes exceeds a specific value and creates a barrier against electron transfer between the nanotubes.

Hopping mechanism is a phenomenon where the electron is transferred at high speed in comparison with quantum tunneling. If the MWCNT percentage inside the nanocomposite is such that there is a shorter distance between nanotubes, the electron is transferred via the hooping method, as depicted in Figure 11. Hopping phenomenon improves electron transfer in MWCNT inside the nanocomposite [22].

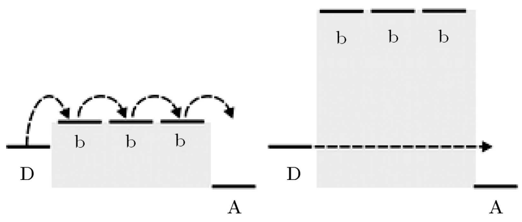

(a) Hopping (b) Tunneling

Figure 11. Electron transfer mechanisms.

According to Figures 12–16, it seems that clusters are formed on the laser line due to falling of MWCNT on the laser line, i.e., when laser temperature exceeds 1500°C [24], part of polymethyl methacrylate found in the laser line is burnt and evaporated and a small part is melted and distributed inside the laser line. The nanotubes found at the limits of the laser line are distributed at the bottom of the laser line since their melting temperature exceeds 3000°C [21] and creates nanotube clusters inside the laser line. Figure 12 depicts images of the electronic microscope of a cross-section of the sample without laser machining.

Comparison of the images of a cross-section of the sample without laser machining depicted in Figure 13 and laser machining lines trace indicates that laser machining of the samples leads to the accumulation of nanotubes inside the laser machined lines, which may be attributed to the increased size of Heat-Affected Zone (HAZ) due to greater heat arising from laser machining and MWCNT fall.

Upon studying images of the electronic microscope of laser machined lines trace presented based on power changes of the machining, it is concluded that increase in power, so much so that it does not result in complete cut of the piece, increases the depth of cut and heat-affected zone. Therefore, more nanotubes fall at the bottom of the laser line appearing in the form of nanotube clusters, and the electrical resistance of the laser line is reduced because power increase leads to greater accumulation and clusters of MWNCT, according to images of the electron microscope.

Moreover, the higher the feed rate of laser machining, the less the depth of laser line cut. Feed rate increase results in cut reduction and thus, few nanotubes are affected while few others fall at the bottom of the laser line. Figure 15 depicts the power of

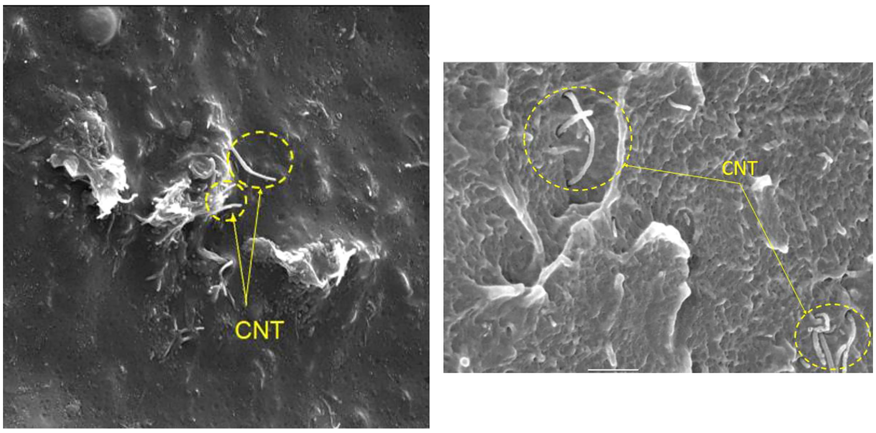

Figure 12. Magnified FE-SEM images from a cross-section of the sample before laser machining.

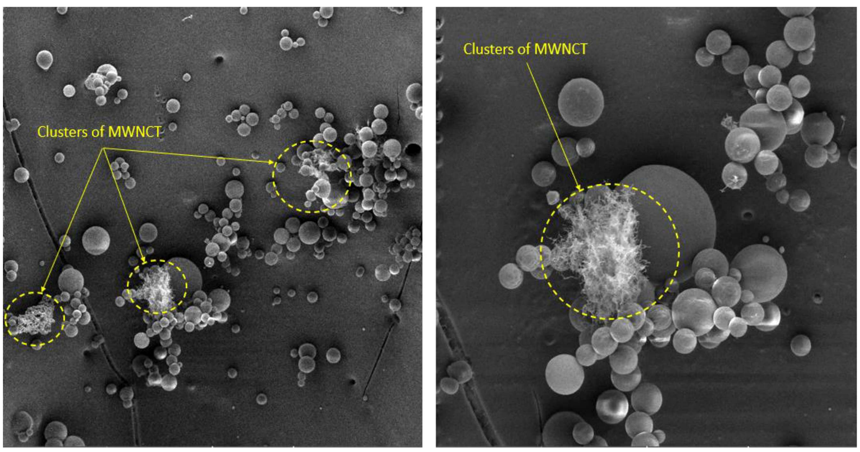

Figure 13. Magnified FE-SEM images of laser machining lines (power of 10 W and feed rate of 75 mm/s).

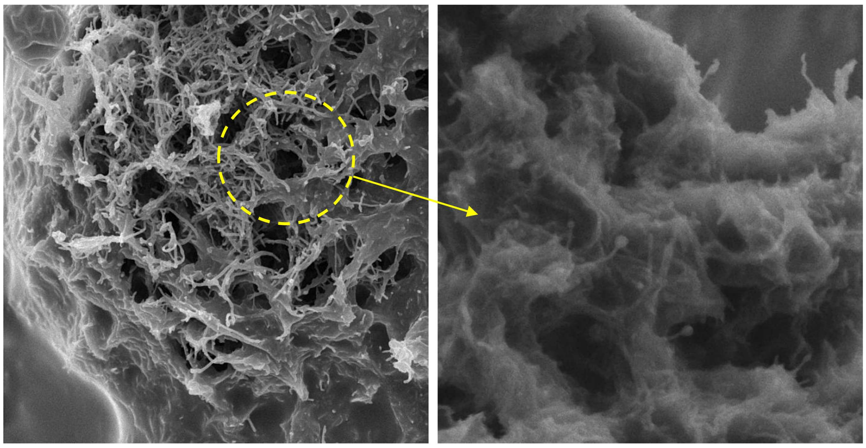

(a) (b)

Figure 14. FE-SEM images of laser machining lines (power of 10 W and feed rate of 75 mm/s): (a) Magnification of 25000 and (b) magnification of 50000.

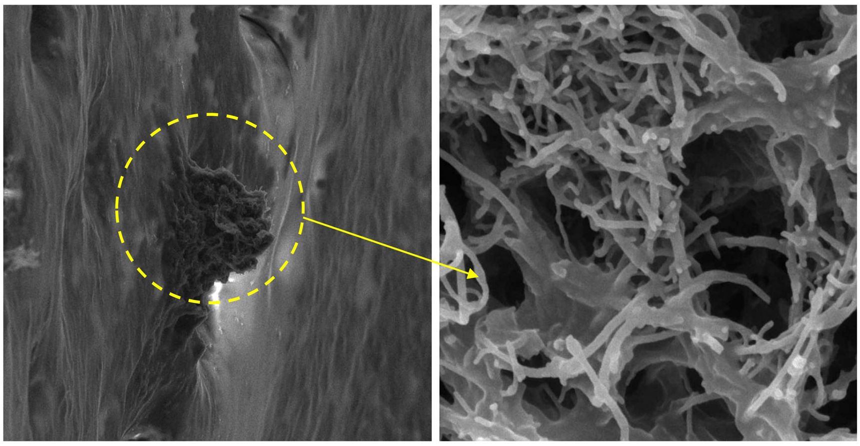

(a) (b)

Figure 15. FE-SEM images of laser machining lines (power of 10 W and feed rate of 75 mm/s): (a) Magnification of 5000 and (b) magnification of 75000.

40 W and feed rate of 15 mm/s where nanotube clusters are presented with more magnification. Figure 16 depicts the power of 40 W and feed rate of 15 mm/s where nanotube clusters are presented. Fixed power of laser machining and increased feed rate resulted in the formation of clusters and nanotube accumulations on a smaller scale.

Figure 17 depicts the average rate diagram for the saturated magnetization parameter. As seen, increase in machining power resulted in the lower reduction of saturated magnetization. The phenomenon may be attributed to temperature increase during the laser machining process. Since laser machining leads to temperature increase by 1500°C at the machining point, magnetic properties of the sample decreased due to temperature increase [25]. Further, an increase in machining power leads to increase in the heat imposed on the piece and increased size of the heat-affected zone [8]. Because of this phenomenon, more MWCNTs are affected by laser heat and the magnetic properties of the nanocomposite are reduced due to increase in machining power. Dispersion of saturated magnetization data is increased due to feeding increase given that the size of the heat-affected zone and cut depth of laser machining is reduced as a result of feed rate increase. Thus, feed rate increase results in much increase in the values of the magnetic properties of composites. Moreover, this increase of magnetic properties is less than that in previous works because both materials constituting nanocomposite have fewer magnetic properties. Moreover, imposing heat on nanocomposites containing MWCNT changes their magnetic structure. These variations are only due to the existence of MWCNT inside the nanocomposite because heat merely reduces the magnetic properties of MWCNT.

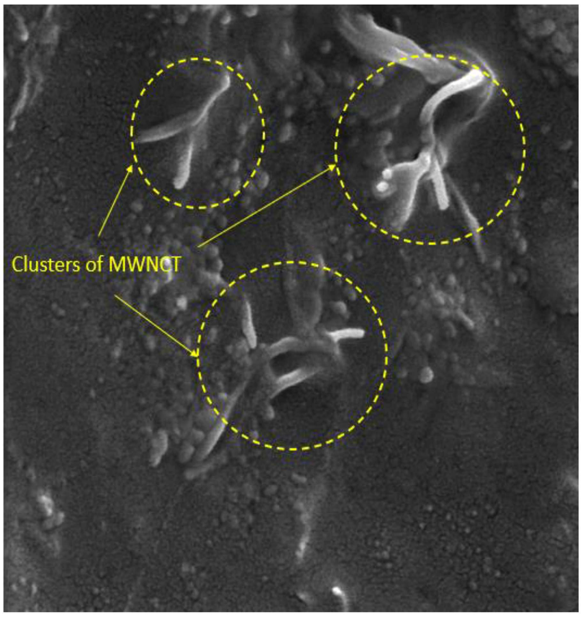

Figure 16. FE-SEM images of laser machining lines (power of 10 W and feed rate of 75 mm/s) with a magnification of 75000.

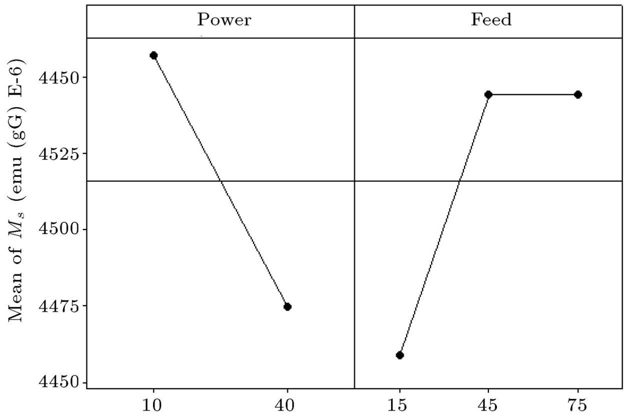

Figure 17. Average rate diagram for M_s parameter.

4. Conclusions

After laser machining of the samples and analysis of variations of their electrical resistance and magnetic properties, the results were obtained as follows:

- Laser machining of the samples decreased electrical resistance in the lasered line on the piece due to the establishment of better relationships between the nanotubes;
- According to variance analysis results, if the laser machining process was implemented using CNC technique, power, feed rate, power × feed rate, and power × angle could physically and statistically affect electrical resistance;
- According to variance analysis results, if the laser machining process was done manually, parameters of power and feed rate would have physical and statistical effects;
- According to the analysis of the signal-to-noise diagrams of machining data using the CNC technique, the levels of 40 W and 15 were ideal levels for power and feed rate parameters, respectively (based on Tables 4 and 5, the effectiveness of the parameters was determined);
- According to the signal-to-noise diagrams of manual impose of angle, optimized levels for power, feed rate, and angle of laser line to the melted flow were 40 W, 15 mm/s, and 0°, respectively;
- Power parameter had physical and statistical effects on saturated magnetization;
- Magnetic properties of the nanocomposites did not change significantly after laser machining.

Acknowledgments

The authors would like to thank Dr. Farshbaf for their unwavering guidance and VSM Laboratory of Birjand.

References

1. Thostenson, E.T., Li, C., Chou, T.W. "Nanocomposites in context", *Compos. Sci. Technol.*, **65**, pp. 491–516 (2005).
2. Taylor, R., Coulombe, S., Otanicar, T., et al. "Small particles, big impacts: A review of the diverse applications of nanofluids", *J. Appl. Phys.*, **113**, pp. 011301–011320 (2013).
3. Lalwani, G., Gopalan, A., DÁgati, M., et al. "Porous three-dimensional carbon nanotube scaffolds for tissue engineering", *J. Biomed. Mater. Res., Part A*, **103**, pp. 3212–3225 (2015).
4. Zhang, X.X., Tejada, J., Hernández, J.M., et al. "Quantum tunneling of the magnetic moment", *Contrib. to Sci.*, ISSN-e 1575-6343, **1**(1), pp. 25–38 (1999).
5. Ghavidel, A.K., Azdast, T., Shabgard, M., et al. "Improving electrical conductivity of poly methyl methacrylate by utilization of carbon nanotube and CO_2 laser", *J. Appl. Polym. Sci.*, **132**, 42671 (2015).
6. Lee, W.J., Lee, S.E., Kim, C.G. "The mechanical properties of MWNT/PMMA nanocomposites fabricated by modified injection molding", *Compos. Struct.*, **76**, pp. 406–410 (2006).
7. Karimzad Ghavidel, A., Azdast, T., Shabgard, M.R., et al. "Effect of carbon nanotubes on laser cutting of multi-walled carbon nanotubes/poly methyl methacrylate nanocomposites", *Opt. Laser Technol.*, **67**, pp. 119–124 (2015).
8. Davim, J.P., Barricas, N., Conceição, M., et al. "Some experimental studies on CO_2 laser cutting quality of polymeric materials", *J. Mater. Process. Technol.*, **198**, pp. 99–104 (2008).

9. Moraczewski, K., Rytlewski, P., Malinowski, R., et al. "Comparison of some effects of modification of a polylactide surface layer by chemical, plasma, and laser methods", *Appl. Surf. Sci.*, **346**, pp. 11–17 (2015).

10. Liebscher, M., Krause, M.B., Pötschke, P., et al. "Achieving electrical conductive tracks by laser treatment of non-conductive polypropylene/polycarbonate blends filled with MWCNTs", *Macromol. Mater. Eng.*, **299**, pp. 869–877 (2014).

11. Gan, X., Fei, G., Wang, J., et al. "Powder quality and electrical conductivity of selective laser sintered polymer composite components", *Struct. Prop. Addit. Manuf. Polym. Components.*, pp. 149–185 (2020) doi:10.1016/B978-0-12-819535-2.00006-5.

12. Yuan, S., Zheng, Y., Chua, C.K., et al. "Electrical and thermal conductivities of MWCNT/polymer composites fabricated by selective laser sintering", *Compos. Part A Appl. Sci. Manuf.*, **105**, pp. 203–213 (2018).

13. Ning, N., Huang, W., Liu, S., et al. "Highly stretchable liquid metal/polyurethane sponge conductors with excellent electrical conductivity stability and good mechanical properties", *Compos. Part B Eng.*, **179**, p. 107492 (2019).

14. Kim, E.J., Lee, C.M. "Experimental study on power consumption of laser and induction assisted machining with inconel 718", *J. Manuf. Process.*, **59**, pp. 411–420 (2020).

15. Kumar Sharma, A., Kumar Jain, P., Vyas, R., et al. "Study of thermal stability and dielectric behavior of PANI/MWCNT nanocomposite", *Mater. Today Proc.*, **38**, pp. 1259–1262 (2021).

16. Wang, L., Qiu, H., Liang, C., et al. "Electromagnetic interference shielding MWCNT-Fe3O4@Ag/epoxy nanocomposites with satisfactory thermal conductivity and high thermal stability", *Carbon N. Y.*, **141**, pp. 506–514 (2019).

17. Kumar, L., Sahoo, S.K., and Alam, S.N. "Effect of xGnP/MWCNT reinforcement on mechanical, wear behavior and crystallographic texture of copper-based metal matrix composite", *Mater. Sci. Eng. B.*, **263**, p. 114888 (2021).

18. Kunde, G.B., Sehgal, B., Ganguli, A.K. "Modified EISA synthesis of $NiAl_2O_4$/MWCNT composite mesoporous free-standing film as a potential electrochemical capacitor material", *J. Alloys Compd.*, **856**, 158019 (2021).

19. Arrechea, S., Guerrero-Gutiérrez, E.M.A., Velásquez, L., et al. "Effect of additions of multiwall carbon nanotubes (MWCNT, MWCNT-COOH and MWCNT-Thiazol) in mechanical compression properties of a cement-based material", *Materialia*, **11**, p. 100739 (2020).

20. Chayad, F.A., Jabur, A.R., and Jalal, N.M. "Effect of MWCNT addition on improving the electrical conductivity and activation energy of electrospun nylon films", *Karbala Int. J. Mod. Sci.*, **1**, pp. 187–193 (2015).

21. Todd, R.H., Allen, D.K., and Alting, L., *Manufacturing Processes Reference Guide*, Industrial Press Inc (1994).

22. Min, C., Shen, X., Shi, Z., et al. "'The Electrical properties and conducting mechanisms of carbon nanotube/polymer nanocomposites: A review", *Polym. Plast. Technol. Eng.*, **49**, pp. 1172–1181 (2010).

23. Ray, S.C., Pao, C.W., Tsai, H.M., et al. "High-temperature annealing effects on multiwalled carbon nanotubes: Electronic structure, field emission and magnetic behaviors", *J. Nanosci. Nanotechnol*, **9**, pp. 6799–6805 (2009).

24. Seidel, G.D. and Lagoudas, D.C. "A micromechanics model for the electrical conductivity of nanotube-polymer nanocomposites", *J. Compos. Mater*, **43**, pp. 917–941 (2009).

25. Gao, G., Çagin, T., and Goddard III, W.A. "Energetics, structure, mechanical and vibrational properties of single-walled carbon nanotubes", *Nanotechnology*, **9**, p. 184 (1998).

26. Ivanova, V.T., Katrukha, G.S., Timofeeva, A.V., et al. "The sorption of influenza viruses and antibiotics on carbon nanotubes and polyaniline nanocomposites", *J. Phys. Conf. Ser.*, **291**, p. 012004 (2011).

Biography

Salar Jabbarpour Azari graduated from the Azad University of Tabriz with a BSc degree in Mechanical Engineering specializing in Manufacturing & Production in 2014. Upon his graduation, he continued his studies and his MSc project in the same field at the same university, which was completed in early 2017.

Mohammadreza Aali received his PhD in Engineering and Science Polymers and Composites from the Institute for Polymers and Composites (IPC) at the University of Minho, Portugal in 2022. His PhD project was related to the computational rheology of thermoplastic polymers. He focused experimentally and numerically on the experimental rheological characterization of polymeric-based materials, particularly the uniaxial extensional rheometry test. He has a numerical and experimental good background in rheometry techniques, material characterization, extensional rheometry flow tests, heat transfer phenomena, viscoelasticity effects on the profile extrusion process for both elastic and viscoelastic fluids, multiphase flows and free-surface topics. Currently, he is a research associate at the IPC. His research interests include rheology, computational rheology, computational modeling, uniaxial extensional rheometry testing, profile extrusion, and polymeric and metallic-based nanomaterials.